

# Biomimetic Total Synthesis and Investigation of the Non-Enzymatic Chemistry of Oxazinin A

Victor Aniebok<sup>+</sup>, Rahul D. Shingare<sup>+</sup>, Hsiao Wei-Lee, Timothy C. Johnstone, and John B. MacMillan\*

**Abstract:** We report the first total synthesis of an antimycobacterial natural product oxazinin A that takes advantage of a multi-component cascade reaction of anthranilic acid and a precursor polyketide containing an aldehyde. The route utilized for the synthesis of the pseudodimeric oxazinin A validates a previously proposed biosynthetic mechanism, invoking a non-enzymatic pathway to the complex molecule. We found a 76:10:9:5 ratio of oxazinin diastereomers from the synthetic cascade, which is an identical match to that found in the fermentation media from the fungus *Eurotiomyces* 110162. Further investigation of the non-enzymatic formation of oxazinin A using <sup>1</sup>H-<sup>15</sup>N HMBC NMR spectroscopy allowed for a plausible determination of the stepwise mechanism. The developed route is highly amenable for the synthesis of diverse sets of analogs around the oxazinin scaffold to study structure–activity relationships (SAR).

There are a growing number of examples of natural products that have been experimentally demonstrated to involve one or more non-enzymatic steps along their biosynthetic pathway.<sup>[1–4]</sup> The complexity of the non-enzymatic step(s) is quite variable, from simple nucleophilic additions to multi-component cyclization cascades. Examples from the latter category, such as homodimericin A,<sup>[5]</sup> the pyonitrins<sup>[6]</sup> and the discoipyrroles<sup>[7]</sup> utilize small reactive functional intermediates to generate complex molecules. The discovery, characterization, and mechanistic study of molecules that undergo these transformations provides new insights into how complex natural products are assembled and strategies for the synthesis of complex natural products, and can provide rapid access to strategies for medicinal chemistry efforts. Oxazinin A (**1**) is a racemic natural

product isolated from a filamentous fungus strain, *Eurotiomyces* 110162, and is shown to have moderate low μM bioactivity against the causative agent of tuberculosis, *Mycobacterium tuberculosis* (Mtb).<sup>[8]</sup> In addition to the promising Mtb activity, we developed an interest in oxazinin A based on a plausible biosynthetic pathway that involves a multi-component, non-enzymatic cascade initiated by an imine (**2**), as shown in Figure 1. As proposed in Figure 1, the fungal biosynthetic machinery produces prenylated polyketide (**3**) and the catabolite anthranilic acid, which come together to form imine **2**, which initiates a cascade intramolecular cyclization as well as an intermolecular dimerization to give oxazinin A.<sup>[8]</sup> Herein, we describe the total synthesis, investigation of stereochemical elements, and a mechanism of formation study around **1**, as well as the creation of structural analogs.

Previously, our laboratory has demonstrated the non-enzymatic formation of the discoipyrroles,<sup>[7]</sup> ammosamides<sup>[2]</sup> and pyonitrins<sup>[9]</sup> via a combination of fermentation studies with labeled substrates, purification of metabolites and/or total synthesis in combination with isotopically labeled substrates coupled with detailed NMR studies. Our NMR studies have taken advantage of an introduced isotope label allowing for the use of heteronuclear NMR experiments with both <sup>13</sup>C and <sup>15</sup>N. In the case of **1**, due to limited access to the producing organism, we have undertaken the investigation of the non-enzymatic formation via total synthesis of the polyketide (**3**).

Synthesis of **3** presented a few challenges, as it required the generation of a penta-substituted aromatic ring with sensitive functionality (Figure 2). In addition to the reactive

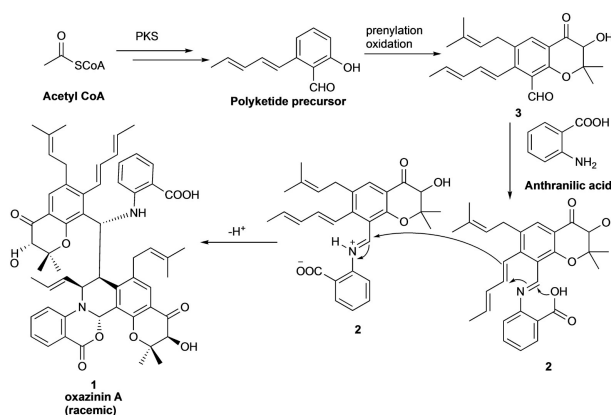


Figure 1. Proposed mechanistic route to oxazinin A.

[\*] Dr. V. Aniebok,<sup>+</sup> Dr. R. D. Shingare,<sup>+</sup> Dr. H. Wei-Lee, Prof. T. C. Johnstone, Prof. J. B. MacMillan  
 Department of Chemistry and Biochemistry, UC Santa Cruz  
 Santa Cruz, CA 95064 (USA)  
 E-mail: jomacmil@ucsc.edu

[†] These authors contributed equally to this work.

© 2022 The Authors. Angewandte Chemie International Edition published by Wiley-VCH GmbH. This is an open access article under the terms of the Creative Commons Attribution Non-Commercial License, which permits use, distribution and reproduction in any medium, provided the original work is properly cited and is not used for commercial purposes.

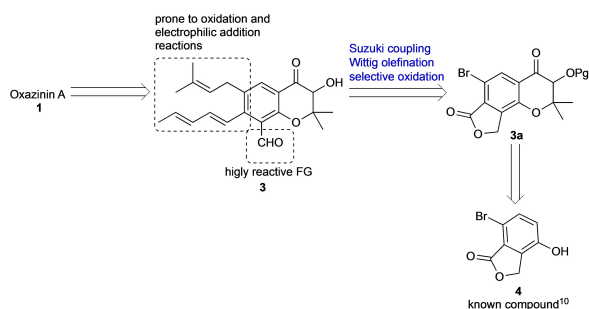
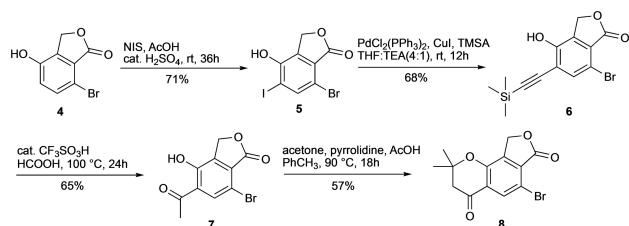


Figure 2. Retrosynthesis of oxazinin A.

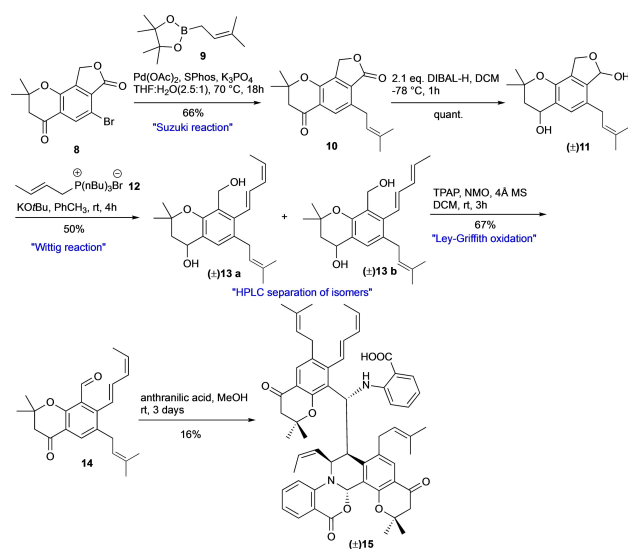
aldehyde, we found the prenyl and pentadiene to be sensitive to a range of electrophiles and oxidative conditions. The reactivity of the aldehyde/diene placed constraints on the synthetic scheme and the relative order of operations. Installation of the chromanone on the right side of the aromatic ring, followed by subsequent  $\alpha$ -oxidation needed to be conducted prior to incorporation of the prenyl group and pentadiene. Accordingly, we planned the synthesis of **3** from the bromolactone (**4**) by employing a key Suzuki cross-coupling, Wittig olefination and a selective oxidation reaction. Intermediate **3a** could be synthesized from a known compound via simple functional group interconversion.

Following Scheme 1, the total synthesis of polyketide **3** began with known bromo-lactone **4**.<sup>[10]</sup> To have a more linear path to **3**, we attempted to introduce the methyl ketone of **7** through traditional acylation methods (e.g., Friedel Crafts acylation/Fries rearrangement), but this did not give an appreciable yield. To circumvent this issue, we first carried out an electrophilic iodination using *N*-iodosuccinimide/acetic acid (**5**), followed by a Sonogashira coupling (**6**),<sup>[11]</sup> and a triflic acid-catalyzed hydrolysis of the silyl acetylene (**7**). The methyl ketone was then cyclized with pyrrolidine/acetone in toluene to give tricyclic intermediate **8** (Scheme 1).

In order to explore the hypothesized cascade cyclization reaction, we further elaborated **8** to give simplified aldehyde precursors **14** and **18**. We performed a Suzuki coupling with **8** and prenyl borate pinacol ester **9**<sup>[12]</sup> to give compound **10** in 66% yield (Scheme 2). Partial reduction of **10** with 2.2 equivalents of di-isobutylaluminum hydride (DIBAL-H) led to reduction to lactol and secondary alcohol **11**.<sup>[13]</sup> The 1,3-pentadiene (**13**) was installed via Wittig olefination<sup>[14–15]</sup> but gave a 2:1 mixture of *E,Z* (**13a**) and *E,E* (**13b**) stereoisomers of the diene, which were easily separated by HPLC.



Scheme 1. Synthesis of chromanone intermediate.

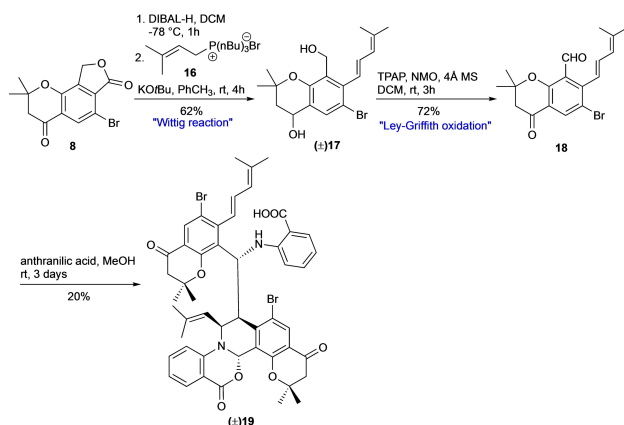


Scheme 2. Synthesis of analog **15**.

The 1,3-diene configuration was ascertained by <sup>1</sup>H NMR using homonuclear decoupling of the terminal methyl group to provide the necessary  $J_{HH}$  values. The two benzylic alcohols of **13a** were oxidized with tetrapropylammonium perruthenate (TPAP) with *N*-methyl morpholine *N*-oxide (NMO) in DCM to form aldehyde **14** in good yield.<sup>[16]</sup> With model compound **14** in hand, we were able to probe the abiotic cascade dimerization. As intermediate **14** was not soluble in water, we pursued the reaction in methanol. Equimolar quantities of **14** and anthranilic acid were allowed to stir for 3 days to give four diastereomers (all racemic) in a ratio of 42:36:14:8 (based on comparing the UV traces via HPLC). The major diastereomer was isolated and the structure determined to be **15** (16% yield) using 1D and 2D NMR spectroscopy; the relative configuration assignment was based on similarity with key chemical shifts and coupling constants reported for **1**.

With one analog and conditions for the late-stage reactions in hand, analog **19**, which contains a geminal dimethyl functionality at the terminus of the diene, was synthesized from intermediate **8** (Scheme 3). Following a DIBAL-H reduction, a Wittig olefination reaction was performed on **8**. To avoid the stereoselectivity problems with the introduction of the diene, the tributyl(3-methylbut-2-en-1-yl)phosphonium bromide **16** was used that gave exclusively the *E* stereoisomer at the newly formed olefin (**17**). After a final oxidation to form the benzylic aldehyde and ketone, the previously optimized dimerization conditions were used to form four diastereomers (in a ratio of 60:27:10:3) of analog **19** (20% yield of the major diastereomer). Although not our primary intention, the bromine handle of this analog was of particular importance as it made the compound more facile to crystallization.

After purification of diastereomers via HPLC, the major diastereomer **19** was crystallized in *n*-hexanes/DCM, and single crystal X-ray diffraction was utilized to get a comprehensive image of the molecule (Figure 3).<sup>[17]</sup> The



**Scheme 3.** Synthesis of analog **19**.

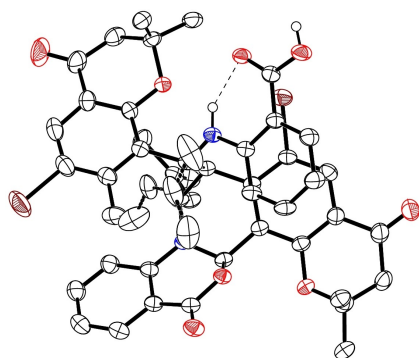


**Figure 3.** Thermal ellipsoid plot (50% probability level) of one of the crystallographically independent molecules of **19**. Non-polar H atoms and minor components of disorder omitted for clarity. Color code: C grey, O red, N blue, Br maroon, H white spheres of arbitrary radius. Intramolecular hydrogen bond shown as a dashed line.

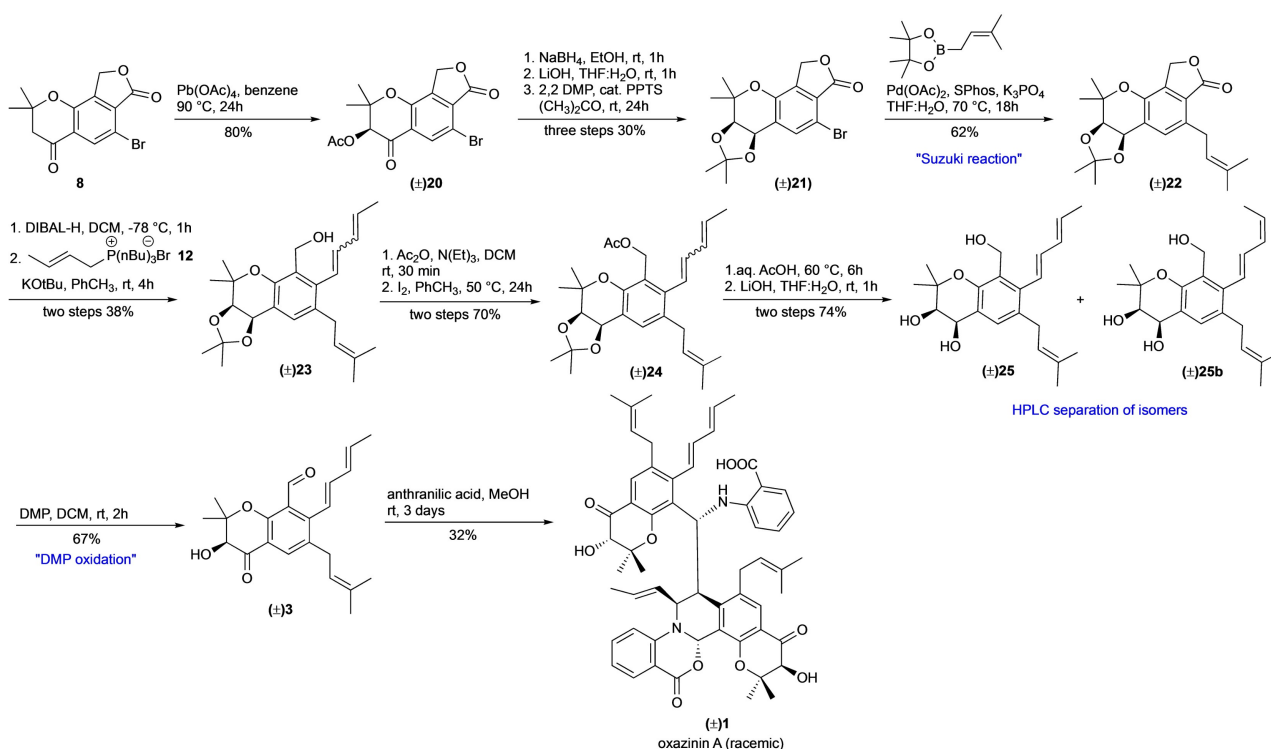
crystal structure showed the major diastereomer was indeed a mixture of two enantiomers, with each enantiomer having the connectivity shown in Scheme 3. This bolstered our confidence in our NMR assignments and the ability to elucidate the non-enzymatic mechanism of oxazinins. While **19** is not as complex as **1**, the relative configuration in the X-ray crystal structure validates the assignment in the isolation.

With these synthetic lessons in hand, the synthesis of **3** was carried out following a similar strategy with slight modifications to accommodate the addition of the secondary alcohol (Scheme 4). From **8**, the  $\alpha$ -position of the chromanone moiety was oxidized with lead tetraacetate ( $\text{Pb}(\text{OAc})_4$ ) to introduce the secondary alcohol and give **20** in 80% yield.<sup>[18]</sup> Next, ketone **20** was reduced ( $\text{NaBH}_4$ ) and the acetoxy moiety was deprotected to afford a diol, which was protected using 2,2-dimethoxypropane and catalytic PPTS in acetone to give acetonide **21** (30% for three steps).<sup>[19]</sup> Compound **23** was subsequently synthesized from **21** via the sequence of Suzuki cross-coupling, DIBAL-H reduction, and Wittig olefination as shown in Scheme 4. We continued to struggle with a mixture of olefin isomers, yielding a 5:1 mixture of  $1E,3Z$  and  $1E,3E$  stereoisomers of the penta-

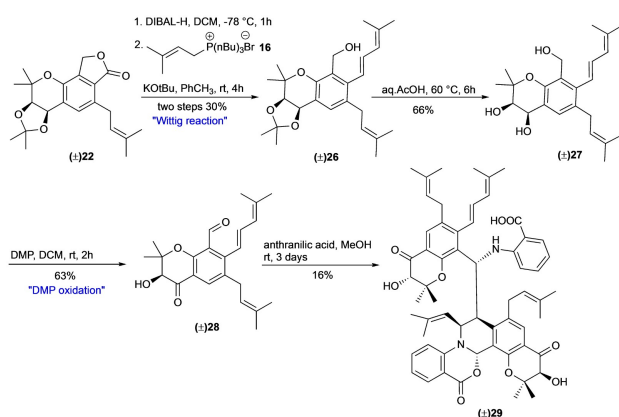
diene **23**. This led to the use of catalytic iodine as a way to convert the  $Z$  stereoisomers to  $E$  stereoisomers. Prior to the iodine-catalyzed diene isomerization reaction, the primary alcohol was protected as an acetate. The mixture of dienes was treated with 0.1 eq of iodine in toluene at  $50^\circ\text{C}$  for 24 h.<sup>[20–21]</sup> This reversed the stereoisomer ratio of **23** to a 1:5 mixture of  $1E,3Z$  and  $1E,3E$  stereoisomers in **24**. The acetonide and  $O$ -acetate protecting groups were removed via treatment with acetic acid (aq.) followed by lithium hydroxide to afford **25a** and **25b** as a mixture of olefins. At this stage we separated the diene isomers by HPLC and unambiguously characterized using homonuclear decoupling NMR spectroscopy.<sup>[22]</sup> Chemoselective oxidation of the two benzylic alcohols of **25a** with Dess–Martin periodinane (DMP) gave the desired aldehyde **3**.<sup>[23]</sup> With aldehyde **3** in hand, addition of anthranilic acid in methanol gave oxazinins **1** (isolated as the major diastereomer in 32% yield) along with three other diastereomers in a ratio of 76:10:9:5 (with an estimated combined yield of ~40%). Importantly, we obtained an LC-MS trace from the original isolation of **1** from the fungal fermentation, which demonstrates a nearly identical ratio of diastereomers (Supporting Information Figure 6). The cascade cyclization/dimerization reaction carried out in a flask, coupled with the resulting diastereomeric mixture comparison with the mixture isolated from the biological system is strong evidence that **1** is the result of an abiotic reaction in the fungal fermentation. Supporting Information Table 1 shows a comparison of the  $^1\text{H}$  and  $^{13}\text{C}$  chemical shifts for synthetic vs isolated **1**. Overall, there is excellent correlation, with small deviations ( $<0.1$  ppm for  $^1\text{H}$  and  $<0.8$  ppm for  $^{13}\text{C}$ ) across the entire molecule.

The growing number of natural products that have been reported to undergo non-enzymatic reactions are often characterized by being isolated as a racemate. In these examples, such as homodimericin<sup>[5]</sup> and discoipyrrole,<sup>[7]</sup> a combination of synthesis and NMR studies have been critical to the validation of the non-enzymatic nature. In the case of **1** the similar diastereoselectivity and racemic nature is strong evidence.

**NMR study:** In order to understand the mechanistic details of oxazinins formation, we have utilized a similar strategy to that used in our mechanistic studies of discoipyrrole,<sup>[7]</sup> wherein we utilized  $^1\text{H}$ - $^{15}\text{N}$  HMBC NMR spectroscopy to monitor for key intermediates formed in real time. We decided to use a more readily available analog of the polyketide which contains a geminal dimethyl group on the terminus of the diene. This was obtained by use of **16** in the Wittig olefination of partially reduced **22**, followed by deprotection and selective oxidation to give aldehyde **28** (Scheme 5). Prior to the NMR study, we carried out the cascade dimerization reaction to obtain **29** and made key NMR assignments. Equimolar equivalents of **28** and  $^{15}\text{N}$ -anthranilic acid (1 eq) were mixed in an NMR tube in methanol- $d_4$  (15.5 mM of **28**), and subjected to an arrayed series of  $^1\text{H}$  and  $^1\text{H}$ - $^{15}\text{N}$  HMBC experiments that were run for durations of 1 min ( $^1\text{H}$ ) and 10 min ( $^1\text{H}$ - $^{15}\text{N}$  HMBC) every 30 minutes for 48 hours. The overall time course of the  $^1\text{H}$ - $^{15}\text{N}$  HMBC was converted into a time-lapse movie with each frame representing one hour (Supplemental movie



**Scheme 4.** Synthesis of oxazinin A from chromanone intermediate **8**.



**Scheme 5.** Synthesis of standard **29** for comparing dimerization reaction.

1). Figure 4a shows a  $^1\text{H}$ - $^{15}\text{N}$  HMBC NMR spectrum of  $^{15}\text{N}$ -labelled anthranilic acid where the  $^{15}\text{N}$  nitrogen appears at  $\delta$   $-311.0$  ppm with strong correlations to the H3 and H6 protons.<sup>[24]</sup> Thirty minutes after the starting materials were added, the formation of **31** is noted. The structure of **31** is assigned based on the chemical shift correlation of protons at  $\delta$  6.23 ppm and  $\delta$  6.83 ppm to  $^{15}\text{N}$  at  $\delta$   $-283.0$  ppm, which correspond to the methine group and aromatic ring of the benzoxazinone, respectively (Figure 4b).

While the dimerization is initiated by Schiff base formation, we were not able to detect a presence of a downfield aldimine  $^{15}\text{N}$  chemical shift in the  $\delta$   $-50$  ppm to  $\delta$   $-200$  ppm range during any of the experiments; this aligns

with the expected transient nature of this initial step. We see the appearance of a new set of cross peaks at  $\delta$   $-299.0$  ppm and  $\delta$   $-293.5$  ppm at 1.5 hours, with the two unique  $^{15}\text{N}$  signals corresponding to the labeled nitrogen atoms in each half of the heterodimer of  $^{15}\text{N}$ -labeled methylated oxazinin analog **32** (Figure 4c). Interestingly, the **32** nitrogen at  $\delta$   $-299.0$  ppm, associated with the isoquinoline ring, showed long range five-bond  $^1\text{H}$ - $^{15}\text{N}$  correlation to the methyl protons attached to the terminal carbon (Figure 4d). This gave us confidence in our assignment of that cross peak. As the reaction proceeds toward product, the intensity of the cross peak at  $\delta$  9.28 ppm and  $\delta$   $-293.5$  ppm increases, which along with peaks at  $\delta$  6.43 ppm,  $\delta$   $-293.5$  ppm and  $\delta$  6.11 ppm,  $\delta$   $-293.5$  ppm, belong to the anthranilic acid moiety of **32**. At 9.5 hours a new peak at  $\delta$  8.23 ppm,  $\delta$   $-165.7$  ppm appears, but it was unclear as to what the identity of that orphan  $^1\text{H}$ - $^{15}\text{N}$  HMBC signal was. We suspect it belongs to  $^{15}\text{N}$ -labeled aldimine **30** but there are no further correlations to support this structure assignment. At around 17 hours the intermediate **31** was consumed and only anthranilic acid, imine intermediate **30** and product **32** remained in the reaction mixture. When the NMR study was stopped after 48 hours there was still unreacted imine and anthranilic acid present in the sample. With this data in hand, we have established a proposed dimerization mechanism (Figure 4f).

The aldimine formed can exist in two activated zwitterionic species: **30**, where the imine nitrogen is protonated and **30'**, where the ketone is protonated. Aldimine **30** can undergo intramolecular attack by the carboxylate to give benzoxazinone **31** (path a). The aldimine **30** and the

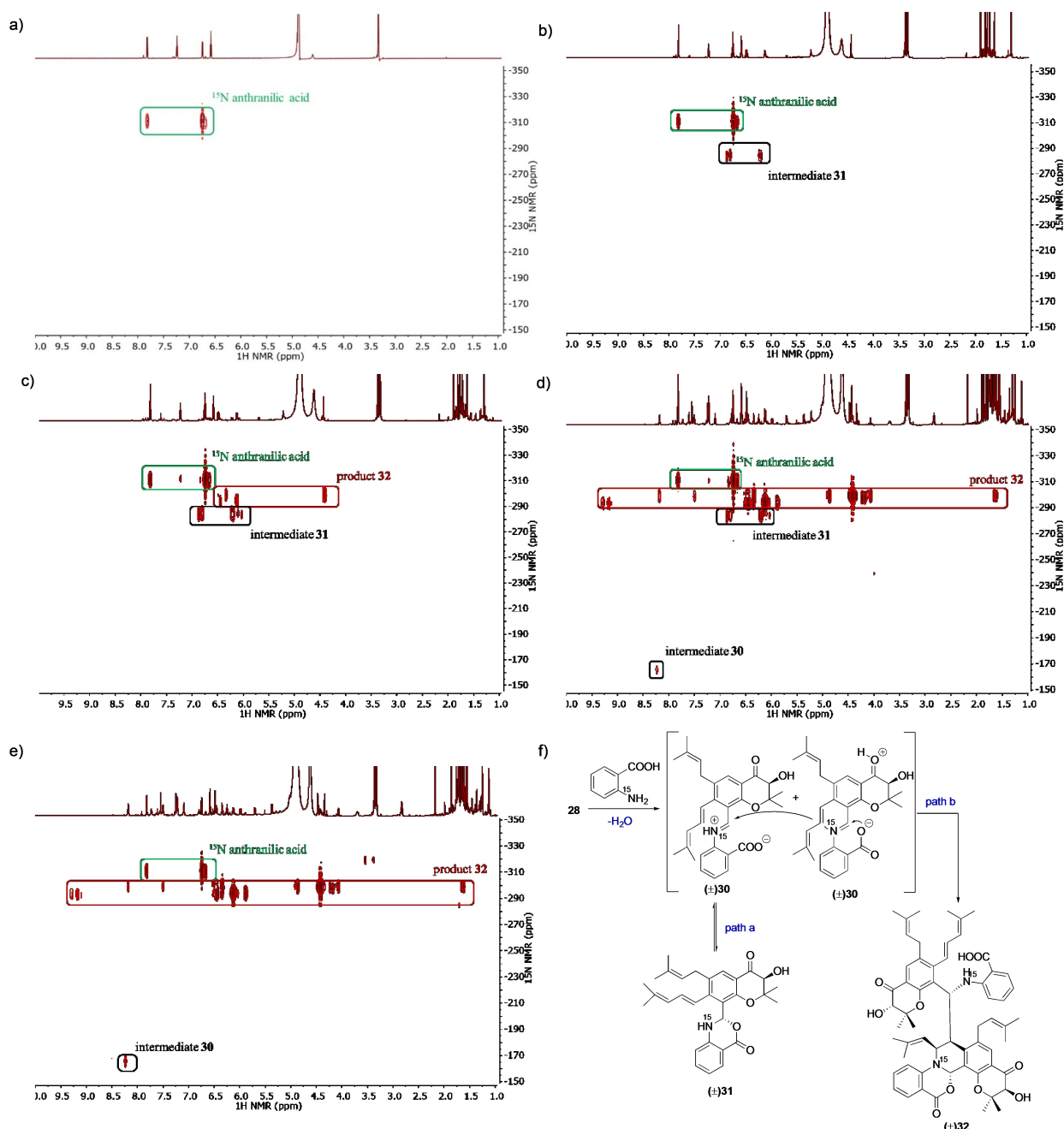
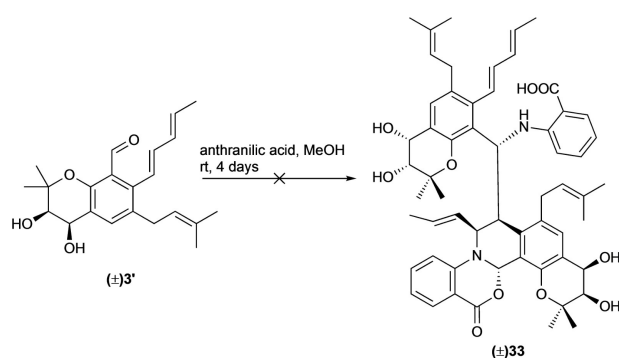


**Figure 4.** a)  $^1\text{H}$ - $^{15}\text{N}$  HMBC of anthranilic acid. b)  $^1\text{H}$ - $^{15}\text{N}$  HMBC of the dimerization reaction at 0.5 hours and formation of **31**. c)  $^1\text{H}$ - $^{15}\text{N}$  HMBC of the dimerization reaction at 1.5 hours and appearance of product **32**. d)  $^1\text{H}$ - $^{15}\text{N}$  HMBC of dimerization reaction at 47.5 hours and appearance of intermediate **30**. e)  $^1\text{H}$ - $^{15}\text{N}$  HMBC of the dimerization reaction at 47.5 hours after significant formation of product **32**. f) Proposed non-enzymatic dimerization mechanism of **28** and anthranilic acid to **32**

benzoxazinone **31** are in an equilibrium as the “open” (aldimine) and “closed” (benzoxazinone) structures, with **31** being the predominant form (as determined by NMR). An equivalent of **30'** initiates the cascade reaction with an initial intramolecular attack by the carboxylate to form the benzoxazinone, followed by a vinylogous Michael addition to form isoquinoline ring and an intermolecular C–C bond formation with imine **30** to give pseudodimer **32** (Figure 4f). Further investigation into this mechanism, including through

theoretical and computational methods are required to understand the diastereoselectivity.

Further, we investigated the role of the chroman-4-one moiety in facilitating dimerization. During the chemoselective DMP oxidation of **25a** to **3** we isolated partially oxidized intermediate **3'** where the primary alcohol was oxidized to an aldehyde and the secondary diols were unreacted (Scheme 6). When this **3'** intermediate was subjected to our standard dimerization conditions, no dimer



**Scheme 6.** Elucidating role of chroman-4-one moiety in dimerization.

formation was observed after 4 days (see Figure S90). This demonstrates that the electron-withdrawing nature of the ketone on the chromanone is crucial for dimerization to occur.

We have completed the first total synthesis and validated the role of non-enzymatic chemistry in the production of the natural product oxazin A. The route to the highly functionalized and oxidatively sensitive aryl aldehyde precursor was highlighted using the lactone as a masked aldehyde for late-stage introduction of the diene sidechain. As demonstrated with the three additional analogs created, the synthetic route is amenable to the generation of a diverse set of analogs for optimizing activity against Mtb.

Oxazin A represents a complex example of the growing number of verified examples of natural products that involve non-enzymatic chemistry as part of their biosynthetic pathway in the producing organism. The mechanistic understanding of the cascade cyclization/dimerization of **1**, as determined by  $^1\text{H}$ - $^{15}\text{N}$  HMBC NMR, provides both a greater understanding of the complex chemistry, with ways to engage key intermediates for further elaboration of the scaffold.

## Experimental Section

Essential Experimental Procedures/Data are in the Supporting Information.

## Acknowledgements

This work was supported by NIH R01CA225960 to JBM. The single-crystal X-ray diffractometer housed in UCSC X-ray Diffraction Facility was funded by NSF MRI grant 2018501. The authors acknowledge Prof. Eric Schmidt (U. Utah) for sharing an authentic sample of oxazin A and an LC-MS trace of the purification of oxazin A from the fungal fermentation.

## Conflict of Interest

The authors declare no conflict of interest.

## Data Availability Statement

The data that support the findings of this study are available from the corresponding author upon reasonable request.

**Keywords:** Non-Enzymatic • Total Synthesis • Biomimetic •  $^1\text{H}$ - $^{15}\text{N}$  HMBC NMR Spectroscopy • 1,3 Diene Isomerization

- [1] P. Fu, A. Legako, S. La, J. B. MacMillan, *Chem. Eur. J.* **2016**, *22*, 3491–3495.
- [2] E. Pan, N. Oswald, J. M. Life, B. A. Posner, J. B. MacMillan, *Chem. Sci.* **2013**, *4*, 482–488.
- [3] Y. Yan, J. Yang, Z. Yu, M. Yu, Y. T. Ma, L. Wang, C. Su, G. P. Horsman, S. X. Huang, *Nat. Commun.* **2016**, *7*, 13083.
- [4] A. W. Robertson, C. M. Martinez-Farina, D. A. Smithen, H. Yin, S. Monro, A. Thompson, S. A. McFarland, R. T. Syvitski, D. L. Jakeman, *J. Am. Chem. Soc.* **2015**, *137*, 3271–3275.
- [5] E. Mevers, J. Saurí, Y. Liu, A. Moser, T. R. Ramadhar, M. Varlan, R. T. Williamson, G. E. Martin, J. Clardy, *J. Am. Chem. Soc.* **2016**, *138*, 12324–12327.
- [6] E. Mevers, J. Saurí, E. N. J. Helfrich, M. Henke, K. J. Barns, T. S. Bugni, D. Andes, C. R. Currie, J. Clardy, *J. Am. Chem. Soc.* **2019**, *141*, 17098–17101.
- [7] D. A. Colosimo, J. B. MacMillan, *J. Am. Chem. Soc.* **2016**, *138*, 2383–2388.
- [8] Z. Lin, M. Koch, M. H. Abdel Aziz, R. Galindo-Murillo, M. D. Tianero, T. E. Cheatham, L. R. Barrows, C. A. Reilly, E. W. Schmidt, *Org. Lett.* **2014**, *16*, 4774–4777.
- [9] R. D. Shingare, V. Aniebok, H.-W. Lee, J. B. MacMillan, *Org. Lett.* **2020**, *22*, 1516–1519.
- [10] K. Ghosh, R. Karmakar, D. Mal, *Eur. J. Org. Chem.* **2013**, *2013*, 4037–4046.
- [11] M. Desroches, M. A. Courtemanche, G. Rioux, J. F. Morin, *J. Org. Chem.* **2015**, *80*, 10634–10642.
- [12] N. Miralles, R. Alam, K. J. Szabo, E. Fernandez, *Angew. Chem. Int. Ed.* **2016**, *55*, 4303–4307; *Angew. Chem.* **2016**, *128*, 4375–4379.
- [13] K. Mikami, H. Ohmura, *Org. Lett.* **2002**, *4*, 3355–3357.
- [14] R. Tamura, K. Saegusa, M. Kakihana, D. Oda, *J. Org. Chem.* **1988**, *53*, 2723–2728.
- [15] L. Catti, K. Tiefenbacher, *Chem. Commun.* **2015**, *51*, 892–894.
- [16] W. P. Griffith, S. V. Ley, G. P. Whitcombe, A. D. White, *J. Chem. Soc. Chem. Commun.* **1987**, 1625–1627.
- [17] Deposition Number CCDC 2171217 (for **19**) contain the supplementary crystallographic data for this paper. These data are provided free of charge by the joint Cambridge Crystallographic Data Centre and Fachinformationszentrum Karlsruhe Access Structures service [www.ccdc.cam.ac.uk/structures](http://www.ccdc.cam.ac.uk/structures).
- [18] M. Tomanik, Z. Xu, S. B. Herzon, *J. Am. Chem. Soc.* **2021**, *143*, 699–704.
- [19] Y. Jung, I. J. Kim, *J. Org. Chem.* **2015**, *80*, 2001–2005.
- [20] S. Hanessian, M. Botta, *Tetrahedron Lett.* **1987**, *28*, 1151–1154.
- [21] G. R. Jachak, P. R. Tharra, P. Sevela, J. Švenda, *J. Org. Chem.* **2021**, *86*, 11845–11861.
- [22] See Supporting Information for detail NMR study.
- [23] G. R. Jachak, P. R. Athawale, H. Agarwal, M. K. Barthwal, G. Lauro, G. Bifulco, D. S. Reddy, *Org. Biomol. Chem.* **2018**, *16*, 9138–9142.
- [24]  $^{15}\text{N}$  chemical shifts to the IUPAC  $\text{CH}_3\text{NO}_2$  standard.

Manuscript received: May 31, 2022

Accepted manuscript online: July 26, 2022

Version of record online: August 16, 2022